Supporting for

Several carbon-coated Ga_2O_3 anodes: Efficient coating of reduced Graphene Oxide enhanced electrochemical performance for lithium ion batteries

Ke Wang*, Wenkai Ye, Weihao Yin, Wenwen Chai, Yichuan Rui and Bohejin Tang[#]

College of Chemistry and Chemical Engineering, Shanghai University of Engineering Science, Shanghai 201620, PR China

[#]Corresponding author: tangbohejin@sues.edu.cn

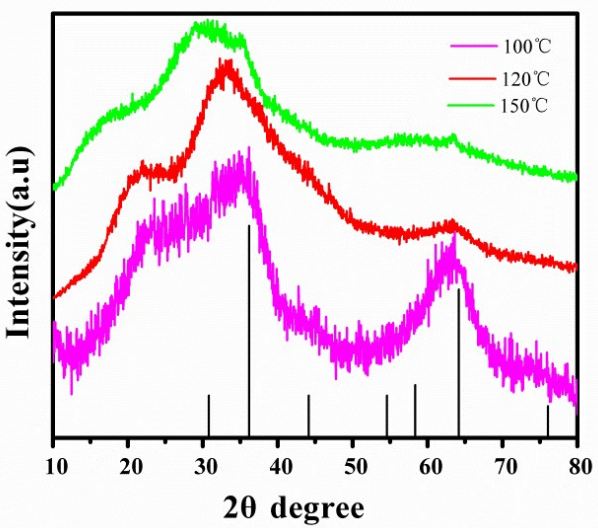

Fig.S1 The XRD pattern of Ga_2O_3 at 100 °C, 120 °C and 150 °C

The XRD pattern of Ga_2O_3 at different temperature was shown in Fig.S1. It can be observed that the XRD pattern of Ga_2O_3 in 100 °C was indexed to the space group (JCPDS#20-0426), which corresponded to the face-centered cubic structure of γ-Ga_2O_3. It is worth noting that with the increase of temperature, the diffraction peak of Ga_2O_3 will shift slightly, but the XRD diffraction peak at 64° of Ga_2O_3 in 120 and 150 °C was still assigned to the Ga_2O_3 (JCPDS#20-0426).

The average particle diameters (*d*) were calculated based on the peak broadening of the

(311) reflection of γ-Ga_2O_3 in 100°C by using the Scherrer formula: $D = \frac{0.89\gamma}{\beta cos\theta}$, $\beta = \frac{X1 - X2}{180} * \pi = 0.0488$, γ=0.15405, $D = 3.87nm$

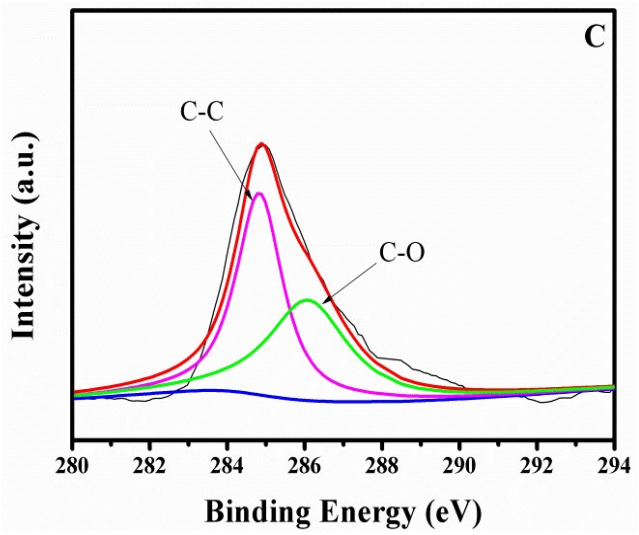

Fig.S2 High-resolution XPS spectrum of C1s.

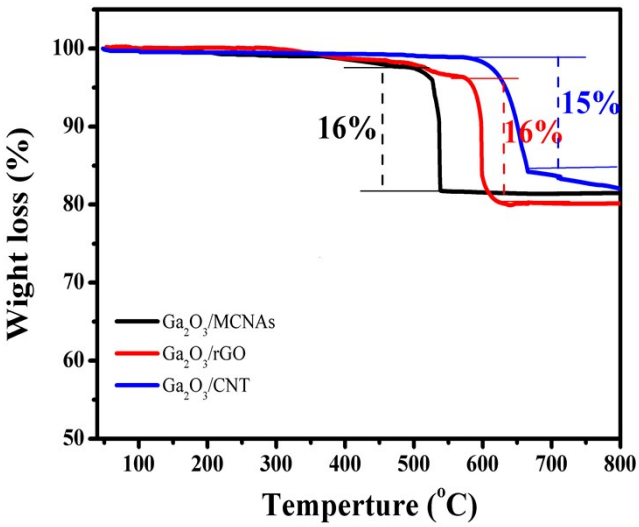

Fig.S3 The TG curves of Ga_2O_3/MCNAs(black line), Ga_2O_3/rGO(red line) ,and Ga_2O_3/CNT(blue line)

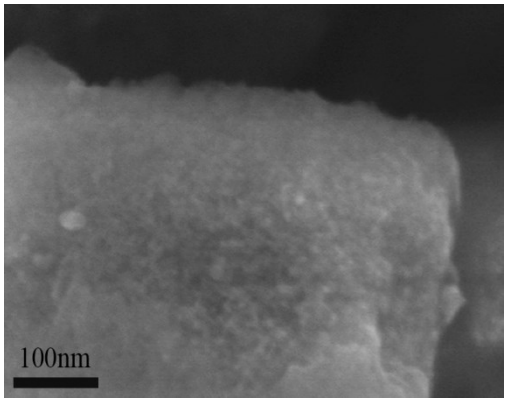

Fig.S4 The SEM image of Ga_2O_3 nanoparticles

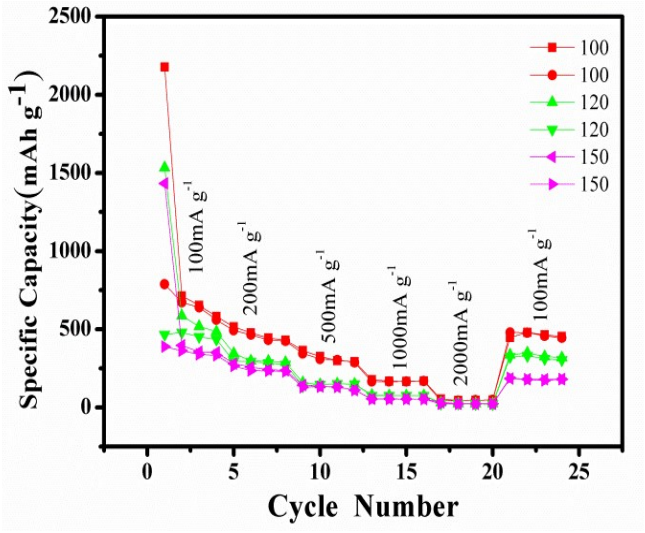

Fig.S5 Rate performance of Ga_2O_3 at three temperatures

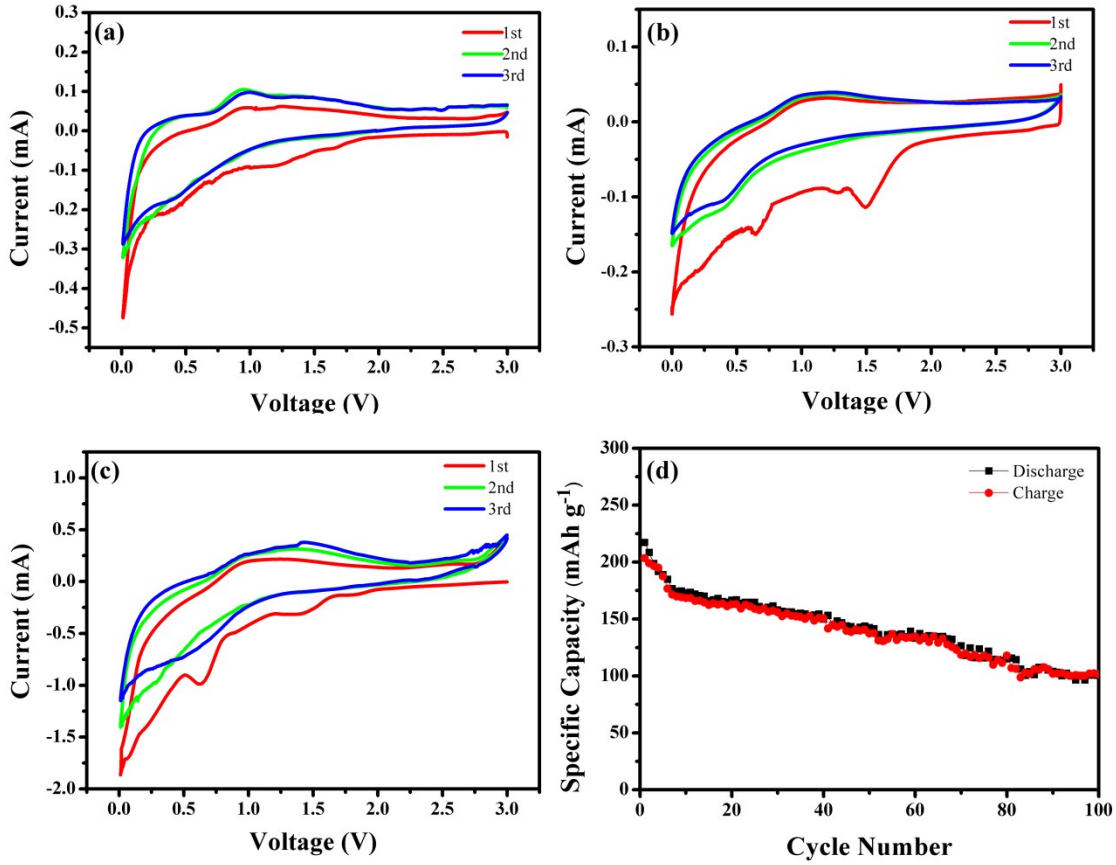

Fig. S6 CV curves of the first three cycles of Ga_2O_3/MCNAs(a), Ga_2O_3/CNT(b) and Ga_2O_3(c) electrodes. (d) Cycling performance of the Ga_2O_3 electrodes at the current density of 1000 mAh g^{-1}

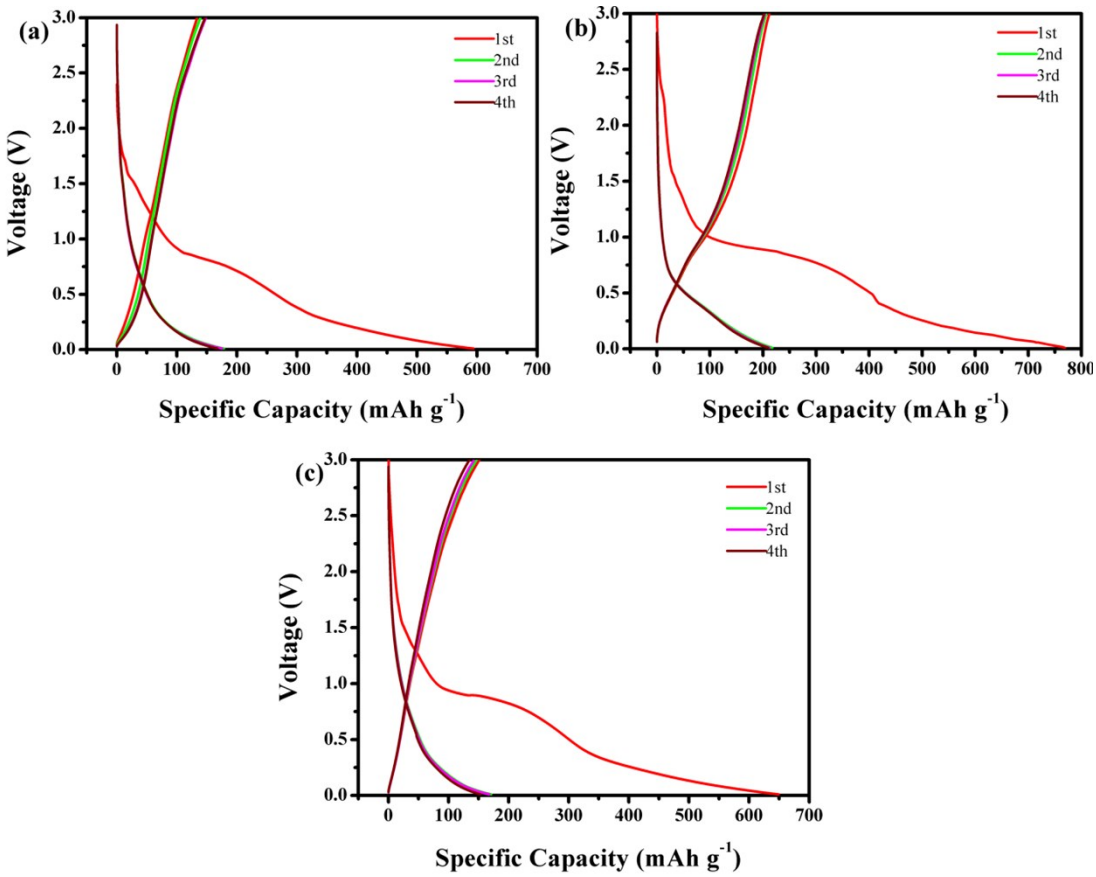

Fig. S7 the galvanostatic charge/discharge curves at 100 mA g^{-1} of rGO (a), MCNAs (b), and CNT(c) electrodes.

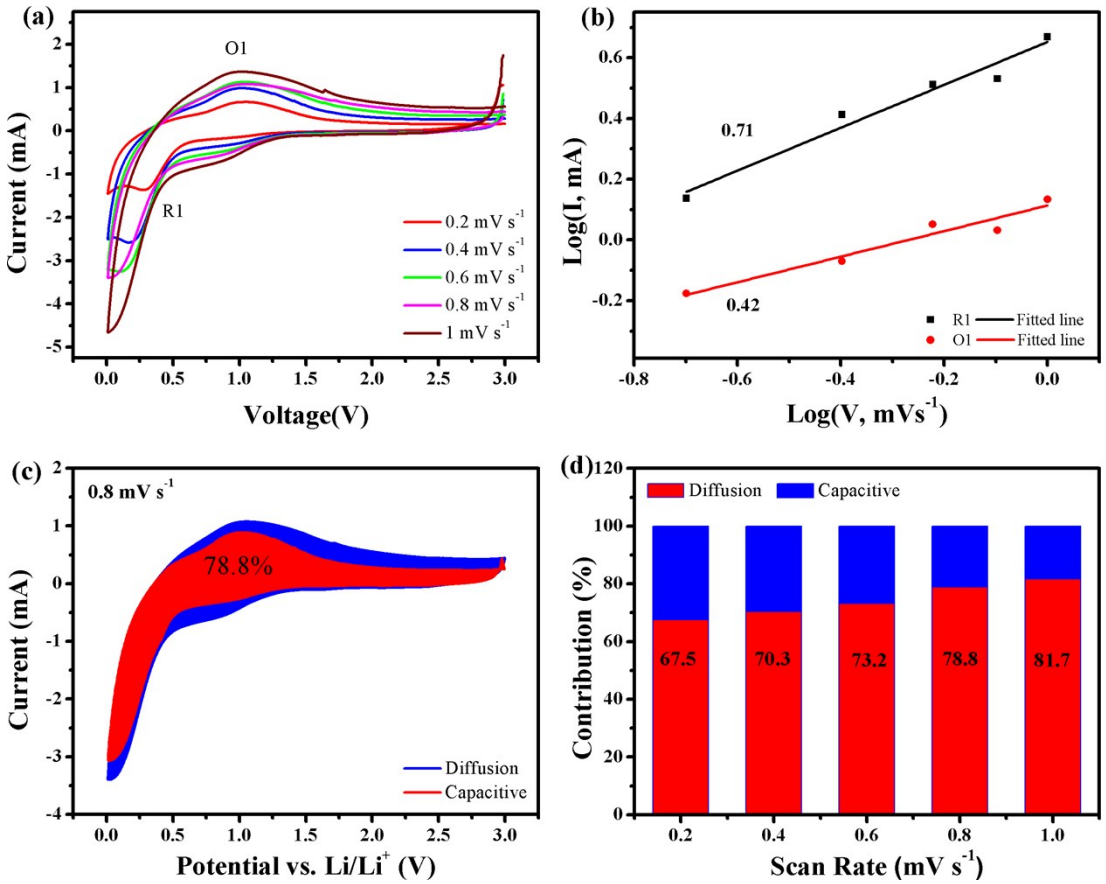

Fig. S8 (a) CV curves at different scan rates ranging from 0.01 V to 3.00 V, (b) relationship of Log i vs. Log v at oxidation and reduction states, (c) capacitive and diffusion contribution to charge storage at 0.6 mV s^{-1}, (d) contribution ratio of the capacitive and diffusion controlled capacities at different scan rates of Ga_2O_3

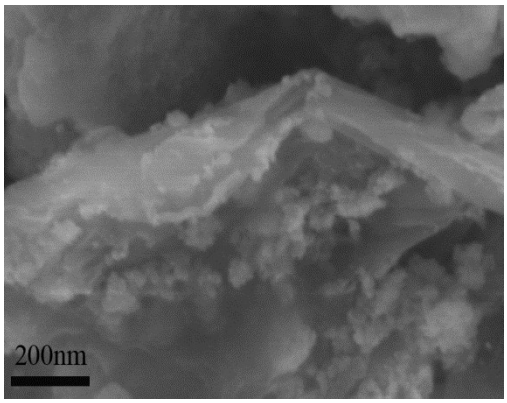

Fig. S9 The SEM image of the Ga_2O_3/rGO electrode after cycling test.

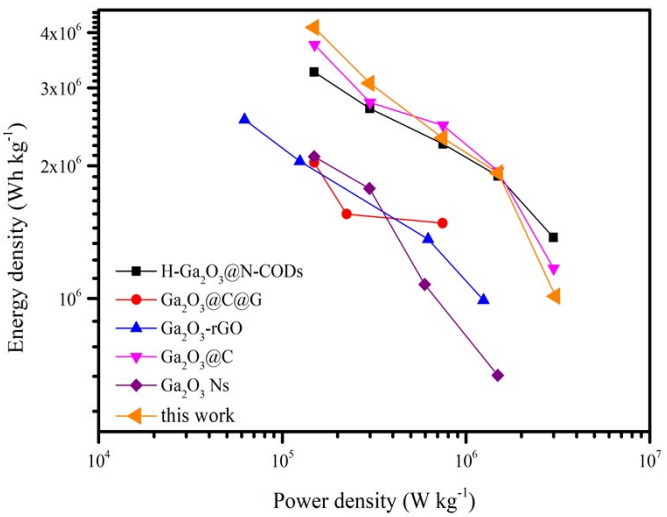

Fig. S10 Ragone plots of different Ga_2O_3 composite materials.

Table.S1 The N_2 adsorption-desorption test results of Ga_2O_3/C and three types of carbon materials.

samples	specific surface area (m^2 g^{-1})	pore volume (cm^3 g^{-1})	pore size (nm)
Ga_2O_3/rGO	253	0.18	2.8
Ga_2O_3/MCNAs	307	0.24	3.4
Ga_2O_3/CNT	293	0.23	3.1
rGO	167	0.16	2.4
MCNAs	1290	1.59	4.2
CNT	187	097	3.7

References

1. J. Guo, F. Gao, D. Li, X. Luo and S. Li, *ACS Sustainable Chemistry & Engineering*, 2020, **XXXX**.
2. S. Ni, Q. Chen, J. Liu, S. Yang, T. Li, X. Yang and J. Zhao, *Journal of Power Sources*, 2019, **433**, 126681.
3. S. B. Patil, I. Y. Kim, J. L. Gunjakar, S. M. Oh, T. Eom, H. Kim and S. J. Hwang, *ACS Appl Mater Interfaces*, 2015, **7**, 18679-18688.
4. X. Tang, X. Huang, Y. Huang, Y. Gou, J. Pastore, Y. Yang, Y. Xiong, J. Qian, J. D. Brock, J. Lu, L. Xiao, H. D. Abruna and L. Zhuang, *ACS Appl Mater*

Interfaces, 2018, **10**, 5519-5526.

5. G. Meligrana, W. Lueangchaichaweng, F. Colò, M. Destro, S. Fiorilli, P. P. Pescarmona and C. Gerbaldi, *Electrochimica Acta*, 2017, **235**, 143-149.